

ARTICLE TYPE

Alternating projection-based iterative learning control for discrete-time systems with non-uniform trial lengths

Zhihe Zhuang¹ | Hongfeng Tao^{*1} | Yiyang Chen^{*2} | Eric Rogers³ | Tom Oomen⁴ | Wojciech Paszke⁵

¹Key Laboratory of Advanced Process Control for Light Industry (Ministry of Education), Jiangnan University, Wuxi, China

²School of Mechanical and Electrical Engineering, Soochow University, Suzhou, China

³School of Electronics and Computer Science, University of Southampton, Southampton, UK

⁴Control Systems Technology Group, Department of Mechanical Engineering, Eindhoven University of Technology, 5612 AZ Eindhoven, the Netherlands

⁵Institute of Automation, Electronic and Electrical Engineering, University of Zielona Gora, Zielona Gora, Poland

Correspondence

*Hongfeng Tao, Key Laboratory of Advanced Process Control for Light Industry (Ministry of Education), Jiangnan University, Wuxi, China. Email: taohongfeng@jiangnan.edu.cn

*Yiyang Chen, School of Mechanical and Electrical Engineering, Soochow University, Suzhou, China. Email: yychen90@suda.edu.cn

Summary

This paper develops a novel framework for iterative learning control (ILC) design of discrete-time systems with non-uniform trial lengths by using the method of alternating projections. In contrast to existing results for the non-uniform trial length problem, this paper uses the Hilbert space setting and hence the linear discrete-time system dynamics with non-uniform trial lengths can be represented by multiple affine subspaces (or linear varieties). Motivated by the successive projection design between two closed convex sets, the considered ILC problem can be transformed into alternating projections between multiple sets, then the Hilbert space setting is used to establish key systems theoretic properties. Moreover, an optimal ILC design is developed for systems with non-uniform trial lengths, which is also extended to the case of input constraints. A numerical case study is given to illustrate the applicability of the new design.

KEYWORDS:

iterative learning control, discrete-time system, alternating projection, non-uniform trial length, input constraint

1 | INTRODUCTION

Iterative learning control (ILC) applies to systems that repeatedly complete the same finite-duration task. An example is a pick-and-place robot performing the following steps: i) collect the payload from a specified location, ii) transfer it over a finite duration, iii) place the payload on a moving conveyor under synchronization, iv) return to the starting location and v) repeat these steps as many times as possible. Let the finite duration be termed the trial length, and use the term trial to denote each

execution. For discrete dynamics, the notation for the system output is $y_k(t)$, $t \in [1, N]$, where both discrete time instant t and trial number k are non-negative integers, and $N < \infty$ denotes the trial length.

Once a trial is complete, all information generated, i.e., for $t \in [1, N]$, is available to update the control signal for the next trial. Let $u_k(t)$, $t \in [0, N - 1]$, $k \geq 0$, denotes the control input on trial k . Then in the ILC setting, suppose that $y_d(t)$, $t \in [1, N]$, is a supplied reference trajectory, e.g., the desired path to be followed by the pick-and-place robot on each trial. In which case the sequence of errors $\{e_k\}_{k \geq 0}$ can be formed, where on trial k , $e_k(t) = y_d(t) - y_k(t)$.

The ILC design problem can now be formulated as the construction of a control input sequence $\{u_k\}_{k \geq 0}$ that enforces convergence from trial-to-trial (k variable) under an appropriate norm to either zero in the ideal case, or to within some acceptable bounds. In ILC, the system input is regulated, and one form of the control law is to construct the control input for the subsequent trial as the sum of that used on the previous trial and a correction based on previous trial information (in some cases, a current trial feedback term is added). The critical feature of ILC is that all information from the prior trial is available to the control law. Hence, for example, an ILC phase-lead law has the structure $u_{k+1}(t) = u_k(t) + \omega e_k(t + \beta)$, $0 \leq \beta \leq N - t$, where the integer $\beta > 0$ denotes the phase-lead action.

The phase-lead term in this last ILC law is implementable because it acts on the previous trial error. If $\beta = 0$, it can be shown that an equivalent feedback control law exists and ILC has no added benefit. Since the mid-1980s, in particular, ILC has remained an active research area, e.g., the first work on robotics¹ and the survey papers.^{2,3} A strong feature of the research is the number of design algorithms that have proceeded to a least experimental validation. Engineering applications include multi-agent systems,^{4,5} printing systems⁶ and center-articulated vehicles.⁷ Also in the process industries, batch processing is amenable to the application of an ILC law.^{8,9}

In most of the ILC literature, the systems are required to track a desired reference trajectory of a fixed finite length and specified a priori. An application area where variable or non-uniform trial lengths arise is in the use of ILC to regulate the level of stimulation applied to patients undergoing robotic-assisted stroke rehabilitation. People who suffer a stroke lose functionality down one side of their body. The recommended method of attempting to recover lost functionality is repeated attempts at a task, e.g., reaching out to an object. However, patients cannot move the affected limb, and the quality of rehabilitation is poor. Muscles can be made to move by applying electrical stimulation to the muscles involved, but regulating the applied stimulation is necessary to achieve maximum effect. In previous work for the upper limb,¹⁰ it was established with supporting clinical trials,¹¹ that ILC can be deployed to regulate the stimulation, where if the patient is improving with each attempt, the voluntary effort should increase, and the applied stimulation decrease. Exactly this effect was detected in the clinical trials.

In the early stroke rehabilitation research, the reference trajectory is chosen based on a healthcare professional's interpretation of the patient's current ability. It must not be too hard (loss of motivation often results) or too easy (no benefit from the session). This early success led to other research on the use of ILC in healthcare, where the trial length is not fixed. One area is the use of

ILC-based functional electrical stimulation to help stroke patients to recover from physiological foot motion. However, for safety reasons or unpredictable voluntary effort by the patient, the stimulation signal must be applied until initial contact is detected between the foot and the ground, which gives rise to an ILC problem of design for non-identical trial lengths.¹² Another area where non-identical, termed non-uniform from this point onwards, trial lengths occur, lies in the filling phase of the injection molding.¹³ The filling phase should be instantly switched to the next phase once the pressure in the molding chamber increases to a certain value, and thus non-uniform trial lengths arise. In response, research has been on ILC design for non-uniform trial lengths.

Early approaches to this last problem include an iterative average operator for improving learning performance using the error and input signals from previous trials.¹⁴ These signals may contain redundant information and affect up-to-date information. To address this issue, more efficient designs were developed, including the searching-compensation mechanisms,¹⁵ the iteratively moving average operator,¹⁶ and the domain alignment operator.¹⁷ A lifted framework, also termed intermittent ILC,¹⁸ was developed for systems with randomly varying trial lengths using the P-type ILC law,¹⁹ for which stronger convergence results were obtained in a stochastic system setting.

In contrast to the random process-based analysis for varying trial length examples, a deterministic convergence property has been developed for tracking ILC design for systems with non-uniform trial lengths in the work of Meng et al.²⁰ Also, a necessary and sufficient condition for monotonic convergence is established with a simple structure ILC design.²¹ In the work of Jin,²² an ILC design is developed using only previous trial information where convergence is analyzed using a modified composite energy function. Moreover, a robust ILC scheme combined with adaptive design techniques is developed for non-uniform trial length systems with nonparametric uncertainties.²³ Also, an adaptive ILC design is developed for the case under a state alignment condition with varying trial lengths. The bounded convergence property is guaranteed using a barrier composite energy function approach.²⁴

A critical question in ILC performance is the speed of the error convergence and how to increase or accelerate it if required. The above designs focus on improving learning efficiency, which cannot increase the convergence speed. In the work of Ketelhut et al.,²⁵ a modification of the norm optimal ILC design for application to non-uniform trial lengths for application to ventricular assist devices. However, this work has no theoretical proof of the feasibility of optimal ILC applied to the non-uniform trial lengths. Also, an intermittent optimal learning control scheme has been developed,²⁶ which aims to achieve fast convergence speed by minimizing a performance index.

Convergence analysis of ILC designs for the non-uniform trial length problem is also a significant issue. Previous approaches to this problem include contraction mapping-based method^{14,16,27} and the Lyapunov-based composite energy function method.^{22,23,24} This paper develops a new design and analysis setting for discrete-time systems with non-uniform trial lengths. In particular, a Hilbert space setting for analysis is used. The Hilbert space setting can simplify the design and analysis

of complex ILC analysis using operator theory. See the work of Owens et al.²⁸ for a comprehensive treatment of the background on the use of Hilbert spaces in ILC analysis and design. The alternating projection method for ILC analysis and design which is also termed successive projection,^{29,30} has been developed for constant trial length systems and extended to the non-uniform trial length case by utilizing the mathematical expectation for only two projecting sets.³¹ This paper extends the alternating projection ILC framework to the non-uniform trial length case by introducing more than two sets, i.e., a finite number of sets, to obtain stronger convergence results in a deterministic setting. Moreover, this paper extends the method of alternating projections in a Hilbert space.

This paper develops an optimal ILC design using the modified alternating projection framework for discrete-time multiple-input multiple-output (MIMO) linear systems with non-uniform trial lengths. Multiple affine subspaces (or linear varieties) represent the discrete-time system dynamics with non-uniform trial lengths. Then, the result of alternating projections between multiple sets can be modified for the optimal ILC design and convergence analysis. In this case, causal implementation is allowed using the norm optimal setting with appropriate modifications. Furthermore, the ILC design is extended to the case of non-uniform trial lengths where input constraints arise or must be imposed for applications-specific reasons. In all cases, the error convergence properties are analyzed. Finally, a numerical case study based on a model obtained from a coarse-fine stage is given to demonstrate the applicability of the new design. The significant novel contributions of this paper are:

- An ILC design framework is developed for discrete-time systems with non-uniform trial lengths using alternating projections between a finite number of sets.
- A causal feedback plus feedforward design for discrete-time systems with non-uniform trial lengths is developed with a strict convergence proof.
- The alternating projection framework is extended to the design for non-uniform trial length examples with input constraints.

The structure of this paper is organized as below. The problem formulation is first addressed in Section 2. Section 3 develops an ILC design for non-uniform trial lengths using alternating projections, and a causal feedback plus feedforward structure is derived for practical implementation. Section 4 gives the new results for input constraints. A numerical case study is provided in Section 5, and the conclusions are in Section 6.

Throughout this paper, \mathbb{N} denotes the set of natural number; \mathbb{R}^n and $\mathbb{R}^{n \times m}$ denote the sets of n -dimensional real vectors and $n \times m$ real matrices, respectively; $l_2^m[a, b]$ denotes the space of \mathbb{R}^m valued Lebesgue square-summable sequences defined on an interval $[a, b]$; The superscripts T and \perp respectively denote the transpose and the orthogonal complement operations; $x \perp y$ represents that x and y are orthogonal; $\mathbf{0}$ denotes zero vector with compatible dimensions; $P_M(x)$ denotes the projection of x onto

the set M in a Hilbert space; \cap denotes the intersection of sets; $\langle \cdot \rangle$ and $|\cdot|$ respectively denote the inner product and determinant, and $\mathbb{X} \times \mathbb{Y}$ denotes the Cartesian product of two spaces \mathbb{X} and \mathbb{Y} . Additional notation will be introduced when required.

2 | PROBLEM FORMULATION

Consider a linear time-invariant discrete-time MIMO system with non-uniform trial lengths described in the ILC setting by the state-space model

$$\begin{cases} x_k(t+1) = Ax_k(t) + Bu_k(t), \\ y_k(t) = Cx_k(t), \end{cases} \quad (1)$$

where $k \in \mathbb{N}$ and $t \in [0, N_k]$ respectively denote the trial number and time index. N_k is a random variable that represents the actual trial length of trial k . $x_k(t) \in \mathbb{R}^n$, $u_k(t) \in \mathbb{R}^l$ and $y_k(t) \in \mathbb{R}^m$ denote the state, input and output vectors, respectively. It is assumed that $|CB| \neq 0$ and therefore the relative degree is equal to one. Without loss of generality, it is also assumed that $x_k(0) = x_0$ for all trials, i.e., same state initial vector on each trial.

One method for ILC analysis and design for the systems considered is to use the lifted model representation, where the values of a variable are represented by assembling them in order as the entries in a vector, and this vector has a finite dimension due to the finite trial length. In this approach, the error updating from trial-to-trial is governed by a standard difference equation and analyzed by standard discrete linear systems theory. See, e.g., the survey papers,^{2,3} for the background on this approach to ILC design.

The non-uniform trial length case does not follow as a direct generalization of lifted model. Therefore, the actual trial length N_k varies within the set $\{N_m, N_m + 1, \dots, N\}$, where N_m and N respectively denote the minimum and maximum trial lengths that occur in a particular application, for which there are $J = N - N_m + 1$ possible trial lengths. In this case, the lifted model with the same trial length N can be employed, i.e.

$$y_k = Gu_k + d_k, \quad (2)$$

where G and d_k represent the system model and the effect of the initial conditions respectively, i.e.

$$G = \begin{bmatrix} CB & 0 & 0 & \dots & 0 \\ CAB & CB & 0 & \dots & 0 \\ CA^2B & CAB & CB & \dots & 0 \\ \vdots & \vdots & \vdots & \vdots & \vdots \\ CA^{N-1}B & CA^{N-2}B & CA^{N-3}B & \dots & CB \end{bmatrix}, \quad (3)$$

$$d_k = \left[(CA)^T \ (CA^2)^T \ \dots \ (CA^N)^T \right]^T x_k(0), \quad (4)$$

and

$$u_k = [u_k^T(0), u_k^T(1), \dots, u_k^T(N-1)]^T, \quad (5)$$

$$y_k = [y_k^T(1), y_k^T(2), \dots, y_k^T(N)]^T. \quad (6)$$

This paper uses a Hilbert space setting. Let $l_2^\ell[0, N-1]$ and $l_2^m[1, N]$ denote the input and output spaces respectively, with inner products and associated induced norms

$$\langle u, v \rangle_R = \sum_{i=0}^{N-1} u^T(i) R v(i), \quad \|u\|_R = \sqrt{\langle u, u \rangle_R}, \quad (7)$$

$$\langle y, e \rangle_Q = \sum_{i=1}^N y^T(i) Q e(i), \quad \|y\|_Q = \sqrt{\langle y, y \rangle_Q}, \quad (8)$$

where $u, v \in l_2^\ell[0, N-1]$ and $y, e \in l_2^m[1, N]$. $R \in \mathbb{R}^{\ell \times \ell}$ and $Q \in \mathbb{R}^{m \times m}$ are symmetric positive definite weighting matrices. In the case when Q and R are chosen as a positive scalar times the compatibly dimensioned identity matrices, their condition numbers will always be 1. Consequently, there is no influence on the stability of control input when these weighting matrices are adjusted to obtain candidate optimal ILC designs to be assessed for their influence on performance. Define $y_d(t)$ as the desired output or reference trajectory for $t \in [1, N]$ in the lifted model setting, i.e.

$$y_d = [y_d^T(1), y_d^T(2), \dots, y_d^T(N)]^T. \quad (9)$$

One problem for ILC design in the non-uniform trial length case is that the actual output values in y_k on trial k are not known for $t \in [N_k + 1, N]$. The reference trajectory is, however, known and hence it is possible to set

$$y_k(t) = y_d(t), \quad t \in [N_k + 1, N]. \quad (10)$$

In this way, learning efficiency of the lifted model for systems with non-uniform trial lengths along the trial can be maintained when using the tracking error to update the input signal for the next trial.

To describe the tracking error of systems with non-uniform trial lengths, a trial-varying matrix is introduced as

$$F_k = \begin{bmatrix} I_{N_k} \otimes I_m & \mathbf{0} \\ \mathbf{0} & \mathbf{0} \otimes I_m \end{bmatrix}, \quad (11)$$

where I_l denotes the identity matrix with dimensions $l \times l$, and \otimes denotes the Kronecker product. Then, the tracking error can be written as

$$e_k = F_k (y_d - y_k), \quad (12)$$

even though the output at $t \in [N_k + 1, N]$ is unknown. In this sense, the error vectors for different trials belong to different subspaces, which depends on the trial number.

Remark 1. These subspaces that the error vectors belong to are actually subsets of each other, and regarding them as independent subspace one by one is the basis for the new ILC design developed in the next section.

The ILC design objective for problem with non-uniform trial lengths is stated as follows.

Definition 1. The ILC problem is to design an update law

$$u_{k+1} = f(u_k, u_{k-1}, \dots, e_k, e_{k-1}, \dots), \quad (13)$$

to update the input signal for current trial utilizing both trial input and tracking errors that have been already obtained, such that the modified tracking error (12) converges to zero in norm as $k \rightarrow \infty$, i.e.

$$\lim_{k \rightarrow \infty} \|e_k\| = 0. \quad (14)$$

Note that in ILC it is possible to use information from any previous trials to update the control input to be applied on the next trial. However in this work, only the most common case is considered, i.e., only information from the previous trial is used, which has evident advantages in terms of applications.

3 | ILC DESIGN USING ALTERNATING PROJECTIONS

In this section, an ILC design for the systems considered is developed by employing alternating projections.

3.1 | Alternating Projections Interpretation

In the case when missing information of the output on a trial is replaced by the corresponding entries in the reference trajectory, the tracking errors for $t \in [N_k + 1, N]$ are set as zero. Then, the tracking errors of different trials belong to different subspaces in Hilbert spaces, and there are J subspaces.

In this sense, the ILC design problem formulated in Definition 1 is equivalent to iteratively finding a point in the intersection of the following multiple closed affine subspaces

$$M_j = \{(e, u) \in H : e = F_j(y_d - y), y = Gu + d\}, \quad (15)$$

$$M_{J+1} = \{(e, u) \in H : e = 0\}, \quad (16)$$

where $M_j \in \{M_1, M_2, \dots, M_J\}$ and M_{J+1} respectively represent system dynamics and the tracking objective, and $d \in l_2^m[1, N]$. The matrix F_j decides which affine subspace M_j lies in $\{M_1, M_2, \dots, M_J\}$, and is defined as

$$F_j = \begin{bmatrix} I_{N_j} \otimes I_m & \mathbf{0} \\ \mathbf{0} & \mathbf{0}_{(N-N_j)} \otimes I_m \end{bmatrix}, \quad (17)$$

where $N_j = N - j + 1$, for $j \in \{1, 2, \dots, J\}$. In addition, the Hilbert space H is defined as

$$H = l_2^m[1, N] \times l_2^\ell[0, N - 1], \quad (18)$$

with the inner product and associated induced norm

$$\langle (e, u), (y, v) \rangle_{\{Q,R\}} = \sum_{i=1}^N e^T(i) Q y(i) + \sum_{i=0}^{N-1} u^T(i) R v(i), \quad (19)$$

$$\|(e, u)\|_{\{Q,R\}} = \sqrt{\langle (e, u), (e, u) \rangle_{\{Q,R\}}}. \quad (20)$$

The following assumption is required.

Assumption 1. The multiple affine subspaces M_j and M_{J+1} given by (15) and (16) have an intersection region in the Hilbert space H , i.e. $M \cap M_{J+1} \neq \emptyset$, where $M = \bigcap_1^J M_j$.

Assumption 1 guarantees the control objective is achievable, and hence the ILC problem has a solution. Also, due to the existence of the intersection region, there must exist a point $(0, u^*) \in M \cap M_{J+1}$.

Different from successive projections used for the constant trial length case,^{29,30} the method of alternating projections used in this paper considers more than two closed sets in the iterative process for the non-uniform trial length case. Therefore, there may be multiple projection orders, hence the notation $\{j_k\}_{k \geq 0}$ is introduced as a sequence taking values in $\{1, 2, \dots, J\}$, and define a sequence $\{z_k\}_{k \geq 0}$ using

$$z_{k+1} = P_{M_{j_{k+1}}}(z_k), \quad k \geq 0, \quad (21)$$

by choosing an arbitrary initial point $z_0 \in H$.

Definition 2. The sequence $s = \{j_k\}_{k \geq 0}$ taking i infinitely many times is represented by

$$\delta(s, i) = \sup_k [\Delta_{k+1}(i) - \Delta_k(i)] < \infty, \quad (22)$$

where $\{\Delta_k(i) \in \mathbb{N}\}_{k \geq 0}$ is an increasing sequence such that $j_{\Delta_k(i)} = i$ with $\Delta_0(i) = 0$.

Taking i infinitely many times requires that the difference in the projection index between the appearance of i at one time and the next is bounded. With Definition 2, the following lemma is required as a basis for the solution of the ILC problem considered.

Lemma 1. Suppose that M_j , for $j \in \{1, 2, \dots, J\}$, are closed subspaces in a Hilbert space. If the sequence $s = \{j_k\}_{k \geq 0}$ takes every value in $\{1, 2, \dots, J\}$ infinitely many times and there exists a constant S , which is only associated with the sequence s , such that

$$\|z_n - z_m\|^2 \leq S \sum_{k=m}^{m-1} \|z_{k+1} - z_k\|^2, \quad n > m \geq 1, \quad (23)$$

then $\{z_k\}_{k \geq 0}$ converges in norm to the orthogonal projection of z_0 onto $M = \bigcap_1^J M_j$.

Proof. See Appendix A, which, in turn, draws on the original result.³² □

Lemma 1 requires that the sequence $s = \{j_k\}_{k \geq 0}$ takes every value in $i \in \{1, 2, \dots, J\}$ infinitely many times and hence the possibility of converging by choosing an appropriate sequence $\{j_k\}_{k \geq 0}$ taking values in $\{1, 2, \dots, J\}$. However, this is a very strict condition for systems with non-uniform trial lengths, because it is not ensured in practice that actual trial length can take every existent length infinitely many times. Therefore, another assumption is made to relax this condition, while the sequence $\{z_k\}_{k \geq 0}$ still converges.

Assumption 2. M_1 appears infinitely many times in the process of alternating projections between (15) and (16), i.e.

$$\delta(s, 1) = \sup_k [\Delta_{k+1}(1) - \Delta_k(1)] < \infty. \quad (24)$$

Note that M_1 represents the system dynamics with $N_k = N$. Therefore, Assumption 2 demands that the case, whose actual length is the desired one, appears infinitely many times and thus the interval between any two sequential trials with desired length is bounded.

Remark 2. This assumption coincides with the persistent full-learning property²⁰ where the actual trial can extend to the desired length at least once between any fixed finite interval of successive trials. Similarly, the actual number of $\delta(s, 1)$ has no influence on the convergence result of ILC design because it is only the existence of $\delta(s, 1)$ that matters. Nonetheless, the smaller this value, the better the learning performance.

Different from Lemma 1, the convergence analysis of alternating projections between (15) and (16) should further consider the affine subspaces of Hilbert space H , namely, the original point of the Hilbert space H does not naturally belong to the designed affine subspaces. Therefore, a property under a designed projection order is firstly proved to establish the convergence. Denote z^* as a point in the intersection region in Assumption 1, i.e., $z^* = (0, u^*) \in M \cap M_{J+1}$, then the following theorem is established.

Theorem 1. If the projection order satisfies

$$M_{j_k} = \begin{cases} M_j \in \{M_1, M_2, \dots, M_J\}, & k \text{ is odd,} \\ M_{J+1}, & k \text{ is even,} \end{cases} \quad (25)$$

then for any $n > m \geq 1$, there exists

$$\langle z_m - z_n, z^* - z_n \rangle \leq 0. \quad (26)$$

Proof. Using Lemma 2 given in Appendix A, the orthogonal projection operator is idempotent and self-adjoint, and therefore

$$\begin{aligned} \langle z - P_{M_j}(z), P_{M_j}(z) - z^* \rangle &= \langle z - z^*, P_{M_j}(z) - z^* \rangle + \langle z^* - P_{M_j}(z), P_{M_j}(z) - z^* \rangle \\ &= \langle z, P_{M_j}(z) \rangle - \langle z, z^* \rangle + \langle z^*, P_{M_j}(z) \rangle - \langle P_{M_j}(z), P_{M_j}(z) \rangle \\ &= \langle z^*, P_{M_j}(z) \rangle - \langle z, z^* \rangle = \langle P_{M_j}(z^*), z \rangle - \langle z, z^* \rangle = 0, \end{aligned} \quad (27)$$

which yields

$$\|z - P_{M_j}(z)\|^2 = \|z - z^*\|^2 - \|P_{M_j}(z) - z^*\|^2 - 2\langle z - P_{M_j}(z), P_{M_j}(z) - z^* \rangle = \|z - z^*\|^2 - \|P_{M_j}(z) - z^*\|^2. \quad (28)$$

Reformulating (28) by adding the projection index k gives

$$\|z_k - z^*\|^2 - \|z_{k+1} - z^*\|^2 = \|z_k - z_{k+1}\|^2, \quad (29)$$

then

$$\|z_m - z^*\|^2 - \|z_n - z^*\|^2 = \sum_{k=m}^{n-1} \|z_{k+1} - z_k\|^2, \quad (30)$$

for $n > m \geq 1$. When m is odd and n is even, introduce a scalar λ to establish the relationship between z_m and z_n . Then

$$z_n = z_{m-1} + \lambda (z_{m+1} - z_{m-1}), \quad n > m \geq 2. \quad (31)$$

Note that $\|z_k - z^*\|^2$ monotonically decreases as trial k increases by (29), so $z_n \in M_{J+1}$ should be a point on the line segment with endpoints z_{m+1} and z^* in the Hilbert space H , where $z_{m+1} \in M_{J+1}$. Then,

$$\|z_n - z_{m-1}\|^2 = \lambda^2 \|z_{m+1} - z_{m-1}\|^2 \geq \|z_{m+1} - z_{m-1}\|^2, \quad (32)$$

which yields $\lambda \geq 1$. Conversely, when $\|z_n - z_{m-1}\|^2$ converges to 0, it follows that

$$\langle z_n - z_m, z_{m-1} - z_m \rangle = 0, \quad (33)$$

and substituting for z_n using (31) yields

$$\lambda = -\frac{\|z_m - z_{m-1}\|^2}{\langle z_{m+1} - z_{m-1}, z_{m-1} - z_m \rangle} = \frac{\|z_m - z_{m-1}\|^2}{\langle z_{m+1} - z_{m-1}, z_m - z_{m+1} + z_{m+1} - z_{m-1} \rangle} = \frac{\|z_m - z_{m-1}\|^2}{\|z_{m+1} - z_{m-1}\|^2}, \quad (34)$$

since $\langle z_{m+1} - z_{m-1}, z_m - z_{m+1} \rangle = 0$, which is established by similar steps to the proof of (27). Then, it follows that

$$1 \leq \lambda \leq \frac{\|z_m - z_{m-1}\|^2}{\|z_{m+1} - z_{m-1}\|^2}. \quad (35)$$

Moreover, reformulating $\langle z_m - z_n, z^* - z_n \rangle$ yields

$$\begin{aligned}
\langle z_m - z_n, z^* - z_n \rangle &= \langle (z_m - z_{m+1}) + (z_{m+1} - z_n), z^* - z_{m-1} - \lambda (z_{m+1} - z_{m-1}) \rangle \\
&= \langle z_m - z_{m+1}, (1 - \lambda) (z^* - z_{m-1}) \rangle + \langle z_m - z_{m+1}, \lambda (z^* - z_{m+1}) \rangle \\
&\quad + \langle (1 - \lambda) (z_{m+1} - z_{m-1}), (z^* - z_{m-1}) - \lambda (z_{m+1} - z_{m-1}) \rangle \\
&= \langle z_m - z_{m-1} + z_{m-1}, (1 - \lambda) (z^* - z_{m-1}) \rangle - (1 - \lambda) \langle z_{m+1}, z^* - z_{m-1} \rangle \\
&\quad + (1 - \lambda) \langle z_{m+1}, z^* - z_{m-1} \rangle - (1 - \lambda) \langle z_{m-1}, z^* - z_{m-1} \rangle - (1 - \lambda) \lambda \|z_{m+1} - z_{m-1}\|^2 \\
&= (1 - \lambda) \left(\langle z_m - z_{m-1}, z^* - z_{m-1} \rangle - \lambda \|z_{m+1} - z_{m-1}\|^2 \right),
\end{aligned} \tag{36}$$

since $\langle z_m - z_{m+1}, z_{m+1} - z^* \rangle = 0$ and $\langle z_m - z_{m-1}, z_m - z^* \rangle = 0$.

Except for $\lambda = 1$, substituting for λ using $\frac{\|z_m - z_{m-1}\|^2}{\|z_{m+1} - z_{m-1}\|^2}$ also yields $\langle z_m - z_n, z^* - z_n \rangle = 0$ since, in (36),

$$\begin{aligned}
\langle z_m - z_{m-1}, z^* - z_{m-1} \rangle - \lambda \|z_{m+1} - z_{m-1}\|^2 &= \langle z_m - z_{m-1}, z^* - z_{m-1} \rangle - \langle z_m - z_{m-1}, z_m - z_{m-1} \rangle \\
&= \langle z_m - z_{m-1}, z^* - z_m \rangle = 0.
\end{aligned} \tag{37}$$

Note that (36) is a quadratic function with respect to λ with a positive quadratic coefficient, therefore $\langle z_m - z_n, z^* - z_n \rangle \leq 0$ by (35) for $n > m \geq 2$. For $n > m = 1$, using z_2, z_1 and $P_{M_{J+1}}^{-1}(z_1)$ yields the same result, where $P_{M_{J+1}}^{-1}(z_1)$, belonging to M_{J+1} , represents the original orthogonal projection point of z_1 .

When m is even and n is odd, by employing two auxiliary points, i.e., $P_{M_{j_n}}(z_m)$ and $P_{M_{j_n}}^{-1}(z_m)$, the same result for the case when n is even and m is odd can be established. When both m and n are odd or even, (26) holds since $\|z_k - z^*\|^2$ monotonically decreases as the projection index k increases, even though the two affine subspaces may not be same when both m and n are odd. \square

Given Theorem 1, the following convergence result can be established.

Theorem 2. The sequence $\{z_k\}_{k \geq 0}$ converges in norm to the orthogonal projection of z_0 onto $M \cap M_{J+1}$ under the projection order (25).

Proof. It follows from the result in (26) in Theorem 1 that

$$\|z_n - z_m\|^2 = \|z_m - z^*\|^2 - \|z_n - z^*\|^2 + 2 \langle z_m - z_n, z^* - z_n \rangle \leq \|z_m - z^*\|^2 - \|z_n - z^*\|^2, \quad n > m \geq 1, \tag{38}$$

and when combined with (30), it follows that

$$\|z_n - z_m\|^2 \leq \sum_{k=m}^{n-1} \|z_{k+1} - z_k\|^2, \quad n > m \geq 1. \tag{39}$$

Recall that (39) is the condition ensuring that the sequence $\{z_k\}_{k \geq 0}$ converges in norm with $S = 1$ by Lemma 1, while the difference lies in that all $M_j, j \in \{1, 2, \dots, J\}$, that are affine subspaces in Theorem 2.

Since $\|z_k - z^*\|^2$ monotonically decreases as k increases and bounded below by 0 according to (29), it follows that there exists a constant $\gamma > 0$ such that $\lim_{k \rightarrow \infty} \|z_k - z^*\|^2 = \gamma$. Moreover, given a constant $\epsilon > 0$, there exists $k \in \mathbb{N}$ such that $0 \leq \|z_m - z^*\|^2 - \gamma < \epsilon/2$ whenever $m \geq k$ and it also works when it comes to $n \geq k$. Then, it follows from (38) that

$$\|z_n - z_m\|^2 \leq \|z_m - z^*\|^2 - \gamma + \gamma - \|z_n - z^*\|^2 < \epsilon/2 + \epsilon/2 = \epsilon, \quad (40)$$

and hence $\{z_k\}_{k \geq 0}$ converges in norm by the completeness property of Hilbert spaces. For ease of notation, the convergent point is denoted by z_∞ .

Note that M_1 appears infinitely many times as stated in Assumption 2, so there is a convergent sub-sequence $\{z_{\Delta_k(1)}\}_{k \geq 0}$ such that each $z_{\Delta_k(1)} \in M_1$. Therefore, there exists $\langle z_{\Delta_k(1)}, z' \rangle = 0$ for every point $z' \in M_1^\perp$, which gives rise to

$$\langle z_\infty, z' \rangle = \left\langle \lim_{k \rightarrow \infty} z_{\Delta_k(J+1)}, z' \right\rangle = \lim_{k \rightarrow \infty} \langle z_{\Delta_k(J+1)}, z' \rangle = 0, \quad (41)$$

and hence $z_\infty \in M_1$. Since M_{J+1} also appears infinitely many times under the designed projection order (25) with $\delta(s, J+1) = 2$, it follows that $z_\infty \in M_{J+1}$. Then, $z_\infty = (0, u_\infty) \in M_1 \cap M_{J+1}$, where u_∞ is the convergent control input and

$$e = 0 = F_1 (y_d - Gu_\infty - d) = (y_d - Gu_\infty - d), \quad (42)$$

since $F_1 = I_N$ by (17). In the case of M_j , it follows that

$$e = F_j (y_d - Gu_\infty - d) = 0, \quad (43)$$

for each $j \in \{2, 3, \dots, J\}$. Then, $z_\infty = (0, u_\infty) \in M_j$ for every $j \in \{2, 3, \dots, J\}$ and hence $z_\infty \in M \cap M_{J+1}$ since $M = \bigcap_1^J M_j$.

Furthermore, considering the following subspaces to project on in the Hilbert space H yields $z_k - P_{M_{j_{k+1}}}(z_k) \in M_{j_{k+1}}^\perp$. Note also that $z^* \in M \cap M_{J+1}$ and thus $z^* \in M_{j_{k+1}}$, and then

$$\langle z_k - z_{k+1}, z^* \rangle = \langle z_k - P_{M_{j_{k+1}}}(z_k), z^* \rangle = 0, \quad (44)$$

which yields

$$\langle z_0 - z_\infty, z^* \rangle = \lim_{k \rightarrow \infty} \langle z_0 - z_{k+1}, z^* \rangle = \lim_{k \rightarrow \infty} (\langle z_0 - z_1, z^* \rangle + \dots + \langle z_k - z_{k+1}, z^* \rangle) = 0. \quad (45)$$

Hence, $z_0 - z_\infty \in (M \cap M_{J+1})^\perp$. By the projection theorem in Hilbert spaces, z_∞ is the orthogonal projection of z_0 onto $M \cap M_{J+1}$ by $z_0 = z_\infty + (z_0 - z_\infty)$ and the proof is complete. \square

The difference between z^* and z_∞ is that z^* can be any point that exists in $M \cap M_{J+1}$ according to Assumption 1, while z_∞ is the convergent point of the sequence $\{z_k\}_{k \geq 0}$ under the designed projection order (25). Also, z_∞ belongs to $M \cap M_{J+1}$ by Theorem 2. Next, the result of Theorem 2 is used to obtain an ILC law design.

3.2 | Optimal ILC Design and Convergence Analysis

To design an optimal ILC update law, a cost function should be formulated for each trial to reduce the tracking error or other targets. According to the alternating projection interpretation, the distance $\|z_{k+1} - z_k\|$ in Hilbert space H is going to be reduced. Therefore, according to the inner product and associated induced norm (19) and (20), the cost function can be taken as

$$J(u_{k+1}) = \|z_{k+1} - z_k\|^2 = \|e_{k+1}\|_Q^2 + \|u_{k+1} - u_k\|_R^2. \quad (46)$$

Moreover, the norm optimal ILC update law³³ can be employed to handle (46), i.e.

$$u_{k+1} = u_k + G^* e_{k+1}, \quad (47)$$

where G^* denotes the adjoint operator of G in Hilbert space and $I = I_N \otimes I_m$.

Remark 3. Due to the property of adjoint operator, the form of the norm optimal ILC update law (47) is not causal, and therefore is not implementable. It will be shown later in this paper that (47) can be reformulated to enable implementation as a simple feedforward or causal feedback plus the feedforward structure. In particular, note that e_{k+1} is associated with F_{k+1} , i.e., the actual length of current trial as defined in (11), which is unknown in advance when calculating u_{k+1} . Also using the calculation along the time, the causality of varying trial lengths can be ensured without losing useful information from historical data.

The next result establishes that the ILC update law (47) solves the problem given in Definition 1.

Proposition 1. The input sequence $\{u_k\}_{k \geq 0}$ generated by update law (47) iteratively solves the ILC problem with non-uniform trial lengths given in Definition 1.

Proof. With the multiple affine subspaces defined in (15) and (16), the ILC problem with non-uniform trial lengths is transformed into the projection problem onto M_{j_k} , where the alternating sequence $\{M_{j_k}\}_{k \geq 1}$ takes values in the order of $\{M_j, M_{J+1}, M_j, M_{J+1}, \dots\}$ under (25). In this sense, let $\tilde{z} = (\tilde{e}, \tilde{u}) \in M_j$ where $j \in \{1, 2, \dots, J\}$ and $z = (0, u) \in M_{J+1}$. Then, for $j \in \{1, 2, \dots, J\}$,

$$\begin{aligned} P_{M_j}(z) &= \arg \min_{\tilde{z} \in M_j} \|\tilde{z} - z\|_H^2 = \arg \min_{(\hat{e}, \hat{u}) \in M_j} \|(\hat{e}, \hat{u}) - (0, u)\|_{\{Q, R\}}^2 \\ &= \arg \min_{(\hat{e}, \hat{u}) \in M_j} \left\{ \|\hat{e} - 0\|_Q^2 + \|\hat{u} - u\|_R^2 \right\} = \arg \min_{\hat{u}} \left\{ \|\hat{e}\|_Q^2 + \|\hat{u} - u\|_R^2 \right\}, \end{aligned} \quad (48)$$

which is an optimization problem solved by update law (47). Similarly,

$$P_{M_{J+1}}(\tilde{z}) = \arg \min_{\hat{z} \in M_{J+1}} \|\hat{z} - \tilde{z}\|_H^2 = \arg \min_{(0, \hat{u}) \in M_{J+1}} \|(0, \hat{u}) - (\tilde{e}, \tilde{u})\|_{(Q, R)}^2 = \arg \min_{(0, \hat{u}) \in M_{J+1}} \left\{ \|0 - \tilde{e}\|_Q^2 + \|\hat{u} - \tilde{u}\|_R^2 \right\}, \quad (49)$$

whose solution is $\hat{u} = \tilde{u}$ when $(0, \hat{u}) \in M_{J+1}$. In this sense, using (47) to solve (48) and (49) repeatedly means alternating projections under the designed order (25). Therefore, the resulting sequence $\{u_k\}_{k \geq 0}$ generated by update law (47) solves the ILC problem in Definition 1. \square

The convergence of the new design will now be analyzed using the alternating projections of Theorem 2.

According to Assumption 1, there exists a point z^* belonging to the intersection region of the multiple subspaces M_j and M_{J+1} , which means systems with non-uniform trial lengths can eventually operate with zero tracking error. This convergence property is established by the following theorem.

Theorem 3. Given system (1) with initial input u_0 , if Assumption 1 holds, application of the optimal ILC update law (47) results in

$$\lim_{k \rightarrow \infty} u_k = u_\infty, \quad \lim_{k \rightarrow \infty} \|e_k\| = 0. \quad (50)$$

Proof. Since the sequence $\{z_k\}_{k \geq 0}$ converges in norm to $z_\infty = (0, u_\infty)$ under the projection order of (25) by Theorem 2, the distance between each two projections converges to 0. Hence, given the cost function (46), it follows that

$$\lim_{k \rightarrow \infty} \left\{ \|0 - e_k\|_Q^2 + \|u_\infty - u_k\|_R^2 \right\} = 0, \quad (51)$$

which establishes (50) by Assumption 1. \square

Remark 4. Although the norm optimal ILC update law (47) is applied, monotonic convergence property of the modified tracking error in norm cannot be achieved in general because the actual lengths are not identical. However, when k is even, there exists $\langle z_k - z_{k+2}, z_{k+2} - z_{k+1} \rangle = 0$, which can be proved in a similar manner to (27), and it follows that

$$\|z_k - z_{k+1}\|^2 = \|z_k - z_{k+2}\|^2 + \|z_{k+2} - z_{k+1}\|^2 + 2 \langle z_k - z_{k+2}, z_{k+2} - z_{k+1} \rangle \geq \|z_{k+1} - z_{k+2}\|^2, \quad (52)$$

which shows that monotonic performance under (25) in Theorem 2 is possible. When k is odd, however, (52) does not always hold because both z_k and z_{k+2} are not always located in the same affine subspace defined in (15), i.e., each two actual trial lengths of the ILC process are not always identical.

In Theorem 3, the convergence of the ILC design for systems with non-uniform trial lengths is proved under the alternating projection framework. Next, it is shown that the ILC law can be reformulated to allow implementation.

3.3 | Causal Feedback Plus Feedforward Implementation

The following steps compose a causal implementation procedure for the ILC law developed in this paper.

Step 1 Input the system dynamics (1), initial input u_0 , positive definite matrices Q and R and stopping criterion value $\sigma > 0$, and set $k = 0$;

Step 2 Calculate the state feedback matrices $K(t)$ for $t \in [0, N - 1]$ using the Riccati equation

$$K(t) = A^T K(t+1) [I_n + BR^{-1}B^T K(t+1)]^{-1} A + C^T Q C, \quad (53)$$

with the boundary condition $K(N) = 0$;

Step 3 Set $k = k + 1$, then calculate feedforward terms $\xi_{k+1}(t)$ for $t \in [0, N - 1]$ by the difference equation

$$\xi_{k+1}(t) = [I_n + K(t)BR^{-1}B^T]^{-1} [A^T \xi_{k+1}(t+1) + C^T Q e_k(t+1)], \quad (54)$$

with the boundary condition $\xi_{k+1}(N) = 0$;

Step 4 Calculate the control input $u_{k+1}(t)$ until $t = N_k - 1$ by

$$u_{k+1}(t) = u_k(t) + R^{-1}B^T p_{k+1}(t), \quad (55)$$

with

$$p_{k+1}(t) = -K(t) [I_n + BR^{-1}B^T K(t)]^{-1} A \times [x_{k+1}(t) - x_k(t)] + \xi_{k+1}(t), \quad (56)$$

where $p_{k+1}(t)$ is a defined costate vector;

Step 5 Set $u_{k+1}(t) = u_k(t)$ for $t \in [N_k, N - 1]$;

Step 6 If $\|e_{k+1}\| < \sigma$, finish the procedure, otherwise return to Step 3.

Remark 5. Steps 1-6 above compose a practical implementation for systems with non-uniform trial lengths, where there exists an extended setting on the input signal when the current trial is ended prematurely. In this case, this procedure can handle systems with non-uniform trial lengths for some complex situations in practice by adjusting to practical requirements. If no available error information is involved in update, set the input of current trial $k + 1$ to be unchanged for safety or other reasons when $t \in [N_{k+1}, N - 1]$, i.e., $u_{k+1}(t) = u_k(t)$.

Remark 6. In practical applications, the stability of control input will be influenced by the accuracy of system dynamic matrices during the computations of implementation procedure (53)-(56). Introduce an uncertainty operator $\Delta : l_2^m [1, N] \rightarrow l_2^m [1, N]$ to denote the uncertainty model $\hat{G} = (I + \Delta)G$. Then, the measured output trajectory $\hat{y}_k = \hat{G}u_k$ will be different from the

numerically computed outputs $y_k = Gu_k$ where accurate system matrices are assumed to be acquired. Then, it follows that

$$\begin{aligned} u_{k+1} &= u_k + G^* \hat{e}_{k+1} = u_k + G^* (\mathbf{I} + \hat{G}G^*)^{-1} \hat{e}_k \\ &= u_k + G^* (\mathbf{I} + \hat{G}G^*)^{-1} F_k (y_d - \hat{G}u_k) \\ &= \left[\mathbf{I} - F_k G^* (\mathbf{I} + \hat{G}G^*)^{-1} \hat{G} \right] u_k + F_k G^* (\mathbf{I} + \hat{G}G^*)^{-1} y_d. \end{aligned} \quad (57)$$

If the uncertainty operator Δ varies within a certain range, which makes $\left\| \mathbf{I} - F_k G^* (\mathbf{I} + \hat{G}G^*)^{-1} \hat{G} \right\| < 1$ satisfied, then we can derive that the control input converges within a boundary, i.e., the stability of the control input can be ensured.

The calculations of both the state feedback matrix $K(t)$ and the feedforward term $\xi_{k+1}(t)$, respectively in (53) and (54), do not violate the law of causality because they will be computed in reverse chronological order. In the causal implementation procedure Steps 1-6, the boundary conditions $K(N) = 0$ and $\xi_{k+1}(N) = 0$ are given firstly, then $K(N-1)$ and $\xi_{k+1}(N-1)$ are computed and so on recursively. The reverse chronological recursion is employed because the Riccati equation forms a causal feedback plus feedforward implementation for the non-causal lifted ILC update law (47). The next result formally establishes this implementation procedure and its proof is given in Appendix B for brevity.

Proposition 2. The norm optimal ILC update law (47) for systems with non-uniform trial lengths can be implemented using the feedback plus feedforward structure given as Steps 1-6.

Proof. See Appendix B. □

4 | EXTENSION TO INPUT CONSTRAINTS

When considering constraints on the input signal, M_{J+1} may not be a closed subspace but still a closed set. Furthermore, the constrained set is usually convex in practice. Therefore, the convex constraint on the input signal can be embedded into the tracking objective, i.e.

$$M_j = \{(e, u) \in H : e = F_j (y_d - y), y = Gu + d\} \quad (58)$$

$$M_{J+1} = \{(e, u) \in H : e = 0, u \in \Omega\}, \quad (59)$$

where Ω is a closed convex set that represents the input constraints and also $M_j \in \{M_1, M_2, \dots, M_J\}$.

Remark 7. The reason why the input constraints are embedded into M_{J+1} , instead of M_j for $j \in \{1, 2, \dots, J\}$, is that $P_{M_{J+1}}(\tilde{z})$ is equivalent to $P_\Omega(\tilde{u})$ by (49) when finding the projection point on M_{J+1} with input constraints. Conversely, if the input constraints are embedded into M_j , a complex constrained optimization problem has to be solved, see the original work²⁹ for a detailed discussion of this case.

Note that when applying alternating projections between (58) and (59), the projection sequence can still be shown to converge in norm if Assumption 1 still holds. However, the convergent point may not be the orthogonal projection of initial point onto the intersection region. Although faster convergence speed occurs under convergence to the projection of initial point, this property is still ensured when the convergent point belongs to the region. In this case, a theorem for ILC design problem with non-uniform trial lengths under input constraints is established next.

Theorem 4. If M_{J+1} is a closed convex set and Assumption 1 holds, the sequence $\{z_k\}_{k \geq 0}$ converges in norm to a point that belongs to $M \cap M_{J+1}$ under the projection order of (25).

Proof. Due to the convexity of M_{J+1} , there exists

$$\left\langle z_k - P_{M_{J+1}}(z_k), P_{M_{J+1}}(z_k) - z \right\rangle \geq 0, \quad (60)$$

for any $z \in M_{J+1}$. In particular, when k is even, there exists $\langle z_{k+1} - z_{k+2}, z_{k+2} - z_k \rangle \geq 0$, and hence

$$\|z_{k+1} - z_k\|^2 = \|z_{k+1} - z_{k+2}\|^2 + \|z_{k+2} - z_k\|^2 + 2 \langle z_{k+1} - z_{k+2}, z_{k+2} - z_k \rangle \geq \|z_{k+1} - z_{k+2}\|^2. \quad (61)$$

When k is odd, (61) may not always hold because the affine subspaces under the projection order (25) arise, i.e., M_j , instead of just convex sets. In a similar manner to (27), it can be shown that

$$\left\langle z_k - P_{M_j}(z_k), P_{M_j}(z_k) - z' \right\rangle = 0, \quad (62)$$

for any $z' \in M_j$, where $j \in \{1, 2, \dots, J\}$. Therefore, for $z^* \in M \cap M_{J+1}$ and all k , there exists $\langle z_k - z_{k+1}, z_{k+1} - z^* \rangle \geq 0$, which yields

$$\|z_k - z^*\|^2 = \|z_k - z_{k+1}\|^2 + \|z_{k+1} - z^*\|^2 + 2 \langle z_k - z_{k+1}, z_{k+1} - z^* \rangle \geq \|z_k - z_{k+1}\|^2 + \|z_{k+1} - z^*\|^2. \quad (63)$$

Furthermore,

$$\|z_0 - z^*\|^2 \geq \|z_k - z^*\|^2 + \sum_{i=0}^{k-1} \|z_i - z_{i+1}\|^2, \quad (64)$$

and when $k \rightarrow \infty$,

$$\infty > \|z_0 - z^*\|^2 \geq \sum_{i=0}^{\infty} \|z_i - z_{i+1}\|^2. \quad (65)$$

Therefore, when $k \rightarrow \infty$, it follows that

$$\inf_{z \in M_{J+1}} \|z_k - z\| \rightarrow 0, \quad (66)$$

and hence the sequence $\{z_k\}_{k \geq 0}$ converges in norm to a point belonging to $M \cap M_{J+1}$ in the defined finite-dimensional Hilbert space H . \square

Using Theorem 4, an optimal ILC update law for systems with non-uniform trial lengths under input constraints is next established, and consists of two parts. The first part is to find the optimal solution in the absence of the input constraints, i.e.,

$$\tilde{u}_{k+1} = u_k + G^* e_{k+1}, \quad (67)$$

which is consistent with (47) and can be implemented using Steps 1-6 given in the previous section. The second is to project the optimal solution onto the constraint set Ω , i.e.,

$$u_{k+1} = \arg \min_{u \in \Omega} \left\{ \|u - \tilde{u}_{k+1}\|_R^2 \right\}, \quad (68)$$

which could be implemented by introducing the constraints on $u_k(t)$ into Steps 1-6 above.

The next result shows that the ILC problem in Definition 1 can be solved by (67) and (68) in the presence of input constraints.

Proposition 3. The input sequence $\{u_k\}_{k \geq 0}$ generated by update law (67) and (68) iteratively solves the ILC problem with non-uniform trial lengths in Definition 1 under input constraints.

Proof. With the multiple closed sets defined in (58) and (59), the ILC problem can be still transformed into the projection problem onto M_{j_k} with the order of $\{M_j, M_{J+1}, M_j, M_{J+1}, \dots\}$. Similar to the proof of Proposition 1, it follows that

$$P_{M_j}(z) = \arg \min_{\hat{u}} \left\{ \|\hat{e}\|_Q^2 + \|\hat{u} - u\|_R^2 \right\}, \quad (69)$$

for $j \in \{1, 2, \dots, J\}$, which can be solved by (67). Projecting on M_{J+1} gives

$$P_{M_{J+1}}(\tilde{z}) = \arg \min_{(0, \hat{u}) \in M_{J+1}} \left\{ \|0 - \tilde{e}\|_Q^2 + \|\hat{u} - \tilde{u}\|_R^2 \right\} = \arg \min_{\hat{u} \in \Omega} \left\{ \|\hat{u} - \tilde{u}\|_R^2 \right\}, \quad (70)$$

which can be solved by (68). Then, the sequence $\{u_k\}_{k \geq 0}$ generated by the update law (67) and (68) solves the ILC problem in Definition 1 in this case. \square

Although M_{J+1} becomes a closed convex set for the problem considered, the convergence of alternating projections, in the order of (25), can be still guaranteed under Assumption 1. Hence the convergence property of ILC update law (67) and (68) is established as the following theorem.

Theorem 5. In the presence of input constraints, consider a system described by (1) with initial input $u_0 \in \Omega$. If Assumption 1 holds and (67) and (68) are applied, then

$$\lim_{k \rightarrow \infty} u_k = u^*, \quad \lim_{k \rightarrow \infty} \|e_k\| = 0. \quad (71)$$

Proof. By Theorem 4 and Proposition 3, although M_{J+1} is a closed convex set, the sequence $\{z_k\}_{k \geq 0}$ converges in norm to a point that belongs to $M \cap M_{J+1}$ under the application of (67) and (68). Therefore, the distance between each two projections

converges to 0, and hence

$$\lim_{k \rightarrow \infty} \left\{ \|0 - e_k\|_Q^2 + \|u^* - u_k\|_R^2 \right\} = 0. \quad (72)$$

By Assumption 1, the convergence of (71) is established. \square

In the presence of input constraints, the specific monotonic performance of Remark 4 for the unconstrained case still exists. Next, a numerical case study is given to illustrate the new results in this paper.

5 | NUMERICAL CASE STUDY

In this section, a coarse-fine stage process is used to verify the effectiveness of the new design. The coarse-fine stage uses multiple actuators, where coarse and fine actuators are respectively in charge of long and short range positioning. High-precision positioning is usually required in many of its practical applications, including some that perform repeating tasks. Therefore, ILC is usually applied to such systems for high tracking performance.³⁴ However, varying trial lengths may happen during the iterative learning process because of some unexpected obstacles in the path or other kinds of output constraints, which gives rise to the non-uniform trial length case. In this simulation, the ILC control problem with non-uniform trial lengths in the control of a coarse-fine stage is considered.

5.1 | Modeling and Design

The employed coarse-fine stage consists of two parts: the coarse stage employs a rotary motor to drive a linear ball-screw stage, and the fine stage is driven by a voice coil actuator. The outputs of the two stages are the position relative to the ground. Denote by the superscript (\cdot) the components of a vector. Then the inputs and outputs of the coarse and fine stages can be denoted by $u^{(1)}$, $y^{(1)}$, $u^{(2)}$ and $y^{(2)}$, respectively. The transfer functions from $u^{(1)}$ to $y^{(1)}$, $u^{(1)}$ to $y^{(2)}$, $u^{(2)}$ to $y^{(1)}$ and $u^{(2)}$ to $y^{(2)}$ are as follows:

$$\begin{aligned} P_{11}(s) &= \frac{m_2 s^2 + cs + \ell}{D(s)}, \quad P_{12}(s) = \frac{m_2 s^2}{D(s)}, \quad P_{21}(s) = \frac{cs + \ell}{D(s)}, \quad P_{22}(s) = \frac{m_1 s^2 + bs}{D(s)}, \\ D(s) &= m_1 m_2 s^4 + (bm_2 + cm_1 + cm_2) s^3 + (bc + \ell m_1 + \ell m_2) s^2 + b\ell s, \end{aligned} \quad (73)$$

where m_1 and m_2 respectively denote the masses of the coarse and fine stages, ℓ and c respectively denote the stiffness and viscous damping coefficient between the two stages, and b denotes the coefficient of viscous damping between the ground and the coarse stage. For further details, see the original modeling process.³⁴ The model parameters are as follows:

$$m_1 = 39.3 \text{ kg}, \quad m_2 = 0.5 \text{ kg}, \quad b = 60 \text{ Ns/m}, \quad \ell = 10^5 \text{ N/m}, \quad c = 45 \text{ Ns/m}. \quad (74)$$

Then, the discrete-time MIMO system dynamic matrices $A \setminus B \setminus C$ used for the implementation procedure in Section 3.3 are

$A = \text{diag}\{A_1, A_2, A_3, A_4\}$ and $B = [B_1^T, B_2^T]^T$, where $\text{diag}\{\cdot\}$ denotes a diagonal matrix and

$$A_1 = A_2 = A_3 = A_4 = \begin{bmatrix} -0.0828 & 279.0791 & 423.1491 & 0 \\ -0.0014 & -0.2112 & -1.8002 & 0 \\ 5.8957 \times 10^{-6} & -8.3944 \times 10^{-4} & 0.9838 & 0 \\ 5.3190 \times 10^{-8} & 1.0825 \times 10^{-5} & 0.0099 & 1 \end{bmatrix}, \quad B_1 = B_2 = \begin{bmatrix} -0.0014 & 0 \\ 5.8957 \times 10^{-6} & 0 \\ 5.3190 \times 10^{-8} & 0 \\ 1.9257 \times 10^{-10} & 0 \\ 0 & -0.0014 \\ 0 & 5.8957 \times 10^{-6} \\ 0 & 5.3190 \times 10^{-8} \\ 0 & 1.9257 \times 10^{-10} \end{bmatrix},$$

and

$$C = \begin{bmatrix} 0 & 0.0254 & 2.2901 & 5.0891 \times 10^{-3} & 0 & 0.0254 & 0 & 0 & 0 & 0 & 0 & 0 & 0 & 0 \\ 0 & 0 & 0 & 0 & 0 & 0 & 0 & 0 & 0 & 0 & 2.2901 & 5.0891 \times 10^3 & 0 & 2 & 3.0534 & 0 \end{bmatrix}.$$

This model is controllable and $|CB| \neq 0$.

For the non-uniform trial length case, set the maximum and minimum tracking time of the coarse-fine stage as 2s and 1.8s respectively, which means that the actual length N_k varies from $N_m = 180$ to $N = 200$ with sample time $T_s = 0.01$ s. Note that the new design requires no settings on the distribution of N_k , and a discrete uniform distribution is employed here for simplicity. Without loss of generality, set $x_k(0) = \underbrace{[0 \ \dots \ 0]^T}_n$ and $u_0(t) = [0, 0]^T$, for $t \in [0, N - 1]$. The desired trajectory of the positioning is taken as

$$y_d^{(1)}(t) = y_d^{(2)}(t) = 1.6t^2 \left[1 + \cos\left(\frac{\pi t}{4} - \pi\right) \right], \quad (75)$$

which means the outputs of both coarse and fine stages follow the same paths and the initial positions of the two stages are identical.

5.2 | Simulation Results

The simulation is implemented in MATLAB R2020a. The weighting matrices are firstly selected as $Q = 10000I_m$ and $R = 0.001I_\ell$, respectively. The design is for a total of 20 trials, and the 2nd, 4th and 20th output profiles are shown in Fig. 1. The output of 20th trial can track the desired trajectory for $1 \leq t \leq N_{20}$ and the output of the first few trials are also plotted with their actual trial lengths in Fig. 1. In particular, the outputs of the 4th trial have worse tracking performance during the interval

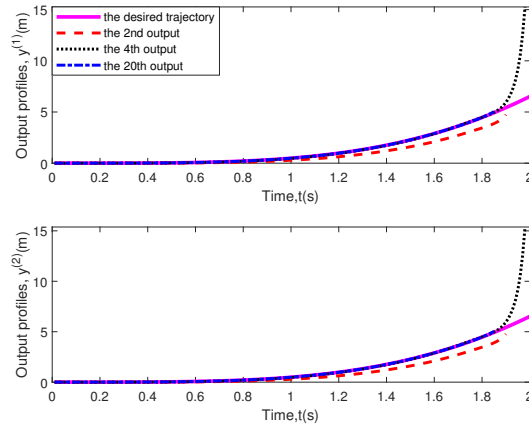


FIGURE 1 The 2nd, 4th and 20th output profiles under the new ILC design with the desired trajectory.

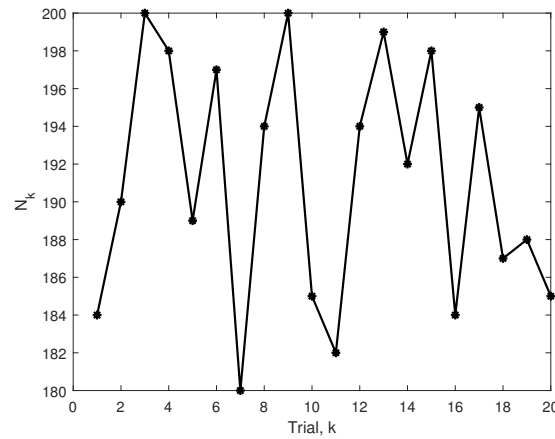


FIGURE 2 The variation of the actual trial lengths.

$[N_k, N]$ and this also possibly occurs at the 20th trial especially when the number of desired length occurs less, which coincides with Remark 2. The variation of the trial lengths is shown in Fig. 2.

The tracking errors in 2-norm along the trial are plotted in Fig. 3, which confirms that the tracking errors can converge asymptotically to zero. For comparison, the ILC method based on an iterative average operator¹⁴ is employed with almost best tuned learning gain $20I_m$, whose tracking errors measured by the 2-norm are also plotted in Fig. 3. Moreover, the P-type ILC method with Arimoto-like gain¹⁹ is also simulated, with learning parameters tuned to $40I_m$. The 2-norm of tracking errors in logarithmic coordinates are also given in Fig. 3. It is evident that the new ILC design converges faster than these two alternatives, because model information is used in the proposed model-based optimal ILC design. The cost function of the new ILC design defined in (46) is given in Fig. 4, and the input increment along the trial is given in Fig. 5 to account for the large values of cost function. The monotonic convergence cannot be obtained because of the non-uniform trial length, which is consistent with the discussion in Remark 4.

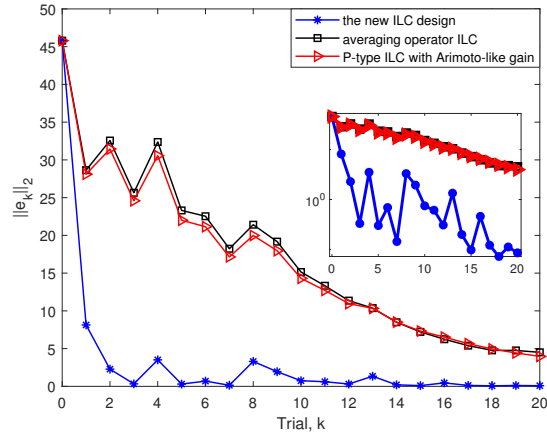


FIGURE 3 The tracking errors in 2-norm of the new ILC design and two alternatives along the trial.

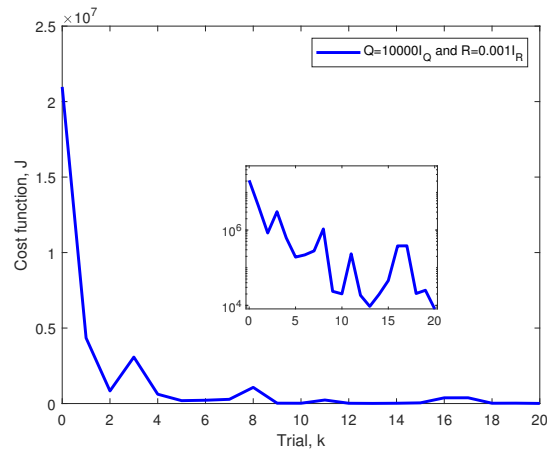


FIGURE 4 The cost function of the new ILC design along the trial.

Different choices of the weighting matrices Q and R can result in different convergence performance of the new ILC design. Fig. 6 gives the results of different Q and R , where increasing Q or decreasing R will result in faster convergence speed. From an intuitive point of view, both Q and R can decide the angle between sets defined in (15) and (16) in Hilbert space H . Changes of the angle will fundamentally affect the results of the convergent sequence $\{z_k\}_{k \geq 0}$ and eventually affect the performance of the new ILC design.

In addition, to check the constraint handling capability, the new ILC design is applied under input constraints. Fig. 7 and Fig. 8 respectively present the 2nd, 4th and 20th output and input profiles with the input constraint $[-3000N, 3000N]$. The actual output can still track the desired trajectory under input constraints after certain trials. The cost function of the new ILC design under the saturation constraint is shown in Fig. 9. It is still convergent and there is less fluctuation along the trials. This phenomenon is due to the varying trial length. The fluctuation of cost function along the trial axis may be decreased since input constraints will restrict the sudden increase caused by varying trial lengths.

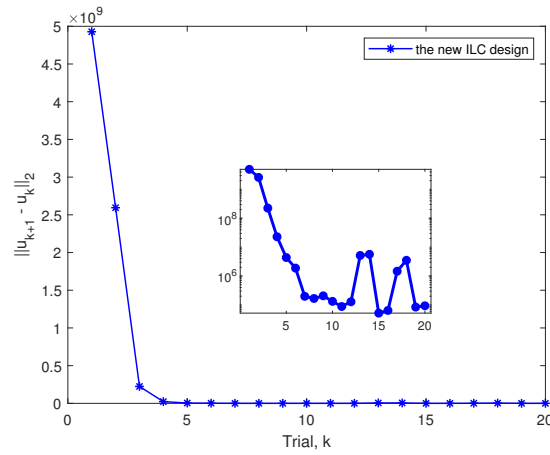


FIGURE 5 The input increment of the new ILC design along the trial.

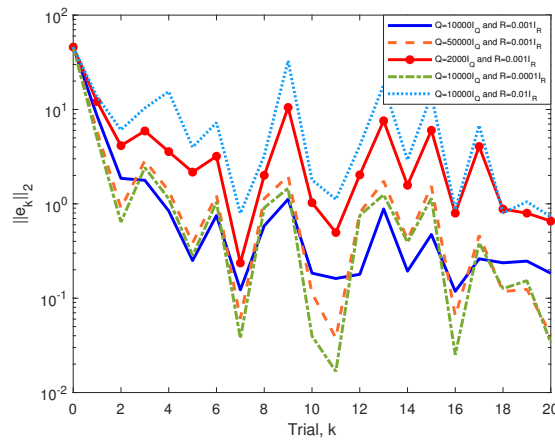


FIGURE 6 The tracking errors in 2-norm of different choices for weighting matrices Q and R .

6 | CONCLUSION AND FUTURE WORK

In this paper, a novel alternating projection framework has been developed for ILC design with non-uniform trial lengths. The causal feedback plus feedforward structure of the uniform norm optimal ILC was modified to give an implementation for discrete-time systems with non-uniform trial lengths. Furthermore, it has been shown that alternating projections for analysis extends to allow input constraints without the need to solve complex optimization problems. Moreover, the convergence properties of the new ILC design were analyzed theoretically. Finally, a numerical simulation based on the model of a coarse-fine stage has been given to demonstrate the effectiveness of the new design for discrete-time systems, including a comparison with two alternative designs, namely, the iterative average ILC and P-type ILC with Arimoto-like gain.

For future work, the ILC design for continuous-time systems with non-uniform trial lengths, where there exists infinite number of sets, will be studied. Furthermore, the new design will be implemented in practice to determine its experimental performance.

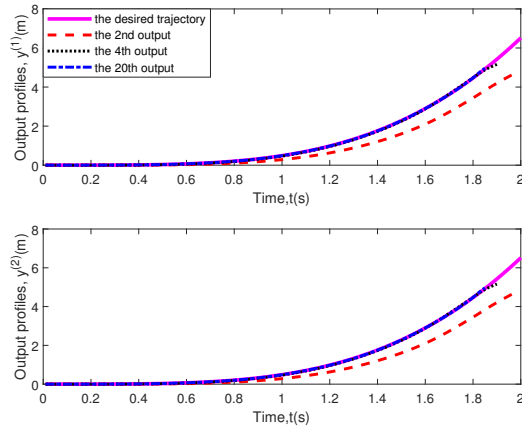


FIGURE 7 The 2nd, 4th and 20th output profiles under the new ILC design with input constraints.

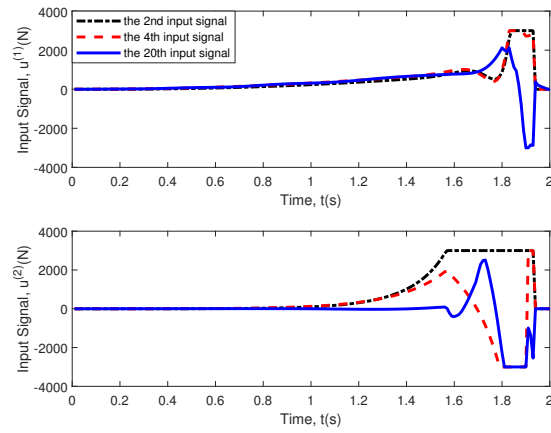


FIGURE 8 The 2nd, 4th and 20th input profiles of the new ILC design with input constraints.



APPENDIX

A PROOF OF LEMMA 1

Before proving Lemma 1, a technical lemma is firstly introduced.

Lemma 2. The projection operator P is idempotent and self-adjoint.

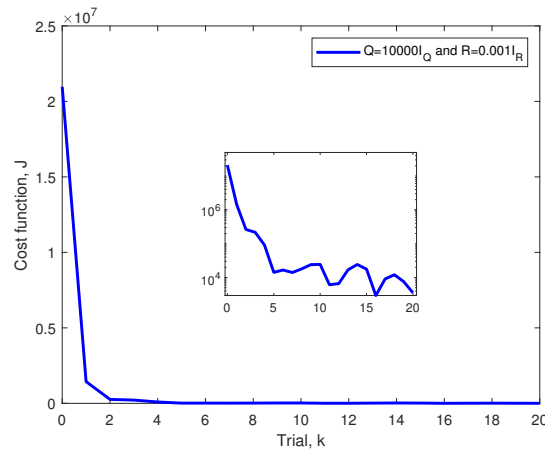


FIGURE 9 The cost function of the new ILC design under input constraints.

Proof. According to the projection theorem in Hilbert spaces, given a Hilbert space H and a subspace $Z \subset H$, each $z \in H$ can be written uniquely as $z = z_1 + z_2$, where $z_1 \in Z$ and $z_2 \in Z^\perp$. Then

$$P_Z^2(z) = P_Z(P_Z(z_1 + z_2)) = P_Z(z_1) = z_1 = P_Z(z), \quad (\text{A1})$$

and the idempotent property is established. Given another $z' \in H$, there exist unique $z'_1 \in Z$ and $z'_2 \in Z^\perp$, then

$$\langle P_Z(z), z' \rangle = \langle z_1, z'_1 + z'_2 \rangle = \langle z_1 + z_2, z'_1 \rangle = \langle z, P_Z(z') \rangle, \quad (\text{A2})$$

and hence the self-adjoint property. \square

Proof of Lemma 1. According to Lemma 2, it follows that

$$\langle P_{M_j}(z), z - P_{M_j}(z) \rangle = \langle P_{M_j}(z), z \rangle - \langle P_{M_j}(z), P_{M_j}(z) \rangle = \langle P_{M_j}(z), z \rangle - \langle P_{M_j}(P_{M_j}(z)), z \rangle = 0, \quad (\text{A3})$$

which yields $z - P_{M_j}(z) \perp P_{M_j}(z)$ and $z_k - z_{k+1} \perp z_{k+1}$ on adding the projection index k . Then, it follows from (A3) that $\|z_k\|^2 = \|z_{k+1}\|^2 + \|z_k - z_{k+1}\|^2$, and by recursion

$$\|z_m\|^2 = \|z_n\|^2 + \sum_{k=m}^{n-1} \|z_{k+1} - z_k\|^2. \quad (\text{A4})$$

Substituting (A4) into (23) gives $\|z_n - z_m\|^2 \leq S(\|z_m\|^2 - \|z_n\|^2)$. Also, it follows from (A4) that $\|z_k\|^2$ is monotonically decreasing and bounded below by 0, and therefore there exists a constant $\alpha \geq 0$ such that $\lim_{k \rightarrow \infty} \|z_k\|^2 = \alpha$. Furthermore, given $\varepsilon > 0$, there exists $k \in \mathbb{N}$ such that $0 \leq \|z_n\|^2 - \alpha < \varepsilon/2S$ whenever $n \geq k$. Therefore,

$$\|z_n - z_m\|^2 \leq S(\|z_m\|^2 - \alpha + \alpha - \|z_n\|^2) < S \cdot \varepsilon/2S + S \cdot \varepsilon/2S = \varepsilon, \quad (\text{A5})$$

and since the sequence $\{z_k\}_{k \geq 0}$ is a Cauchy sequence in Hilbert spaces, $\{z_k\}_{k \geq 0}$ converges in norm to a point, which is denoted by z_∞ .

Since $\{j_k\}_{k \geq 0}$ takes every value in $\{1, 2, \dots, J\}$ infinitely many times, there is a sub-sequence $\{z_{\Delta_k(i)}\}_{k \geq 0}$ such that each $z_{\Delta_k(i)} \in M_j$. Then, there exists $\langle z_{\Delta_k(i)}, z' \rangle = 0$ for every point $z' \in M_j^\perp$, which gives rise to

$$\langle z_\infty, z' \rangle = \left\langle \lim_{k \rightarrow \infty} z_{\Delta_k(i)}, z' \right\rangle = \lim_{k \rightarrow \infty} \langle z_{\Delta_k(i)}, z' \rangle = 0. \quad (\text{A6})$$

Therefore, there exists $z_\infty \in M_j$ for each $j \in \{1, 2, \dots, J\}$, and hence we have $z_\infty \in M = \bigcap_1^J M_j$.

Finally, $z_\infty = P_M(z_0)$ must be established to complete the proof. To show that z_∞ is the orthogonal projection of z_0 onto M , it suffices to show that $z_0 - z_\infty \in M^\perp$, since then

$$z_0 = \underbrace{z_\infty}_{\in M} + \underbrace{z_0 - z_\infty}_{\in M^\perp}, \quad (\text{A7})$$

by the projection theorem in Hilbert spaces. Let $z \in M$, and hence $z \in M_{j_{k+1}}$. Since the projection operator is self-adjoint and idempotent, it can also be proved that $z_k - P_{M_{j_{k+1}}}(z_k) \in M_{j_{k+1}}^\perp$. Then

$$\langle z_k - z_{k+1}, z \rangle = \langle z_k - P_{M_{j_{k+1}}}(z_k), z \rangle = 0, \quad (\text{A8})$$

which yields

$$\langle z_0 - z_\infty, z \rangle = \lim_{k \rightarrow \infty} \langle z_0 - z_k, z \rangle = \lim_{k \rightarrow \infty} (\langle z_0 - z_1, z \rangle + \langle z_1 - z_2, z \rangle + \dots + \langle z_{k-1} - z_k, z \rangle) = 0. \quad (\text{A9})$$

Finally, $z \in M$, hence $z_0 - z_\infty \in M^\perp$, and the proof is complete. \square

B PROOF OF PROPOSITION 2

By the definition of the adjoint, it follows that

$$\langle e, Gu \rangle_Q = e^T \mathbf{QGR}^{-1} \mathbf{R}u = \langle \mathbf{R}^{-1} G^T \mathbf{Q}e, u \rangle_{\mathbf{R}} = \langle G^* e, u \rangle_{\mathbf{R}}, \quad (\text{B10})$$

where $\mathbf{R} = \text{diag}\{\mathbf{R}, \mathbf{R}, \dots, \mathbf{R}\} \in \mathbb{R}^{\ell \cdot N \times \ell \cdot N}$ and $\mathbf{Q} = \text{diag}\{\mathbf{Q}, \mathbf{Q}, \dots, \mathbf{Q}\} \in \mathbb{R}^{m \cdot N \times m \cdot N}$. The update law (47) can now be written as

$$u_{k+1} = u_k + \mathbf{R}^{-1} G^T \mathbf{Q}e_{k+1}, \quad (\text{B11})$$

i.e.

$$u_{k+1}(t) = u_k(t) + \sum_{i=t+1}^N \mathbf{R}^{-1} B^T (A^T)^{i-t-1} C^T \mathbf{Q}e_{k+1}(i). \quad (\text{B12})$$

Then, set $p_{k+1}(t)$ as

$$p_{k+1}(t) = \sum_{i=t+1}^N (A^T)^{i-t-1} C^T Q e_{k+1}(i), \quad (\text{B13})$$

which yields (55), and hence for $t \in [0, N-1]$, $p_{k+1}(t)$ can be computed by the recursion relation

$$p_{k+1}(t) = A^T p_{k+1}(t+1) + C^T Q e_{k+1}(t+1), \quad (\text{B14})$$

with the boundary condition $p_{k+1}(N) = 0$. If it is assumed that the state of system (1) is fully known,³³ there exists a causal implementation with respect to $p_{k+1}(t)$ in the form (56). It now follows from (1), (56) and (B14) that

$$\begin{aligned} x_{k+1}(t+1) - x_k(t+1) &= A [x_{k+1}(t) - x_k(t)] + BR^{-1} B^T p_{k+1}(t) \\ &= [I_n + BR^{-1} B^T K(t)]^{-1} A [x_{k+1}(t) - x_k(t)] + BR^{-1} B^T \xi_{k+1}(t). \end{aligned} \quad (\text{B15})$$

Furthermore, to eliminate $p_{k+1}(t)$, substituting (56) and (B15) to (B14) yields

$$f_1[X, K(t), K(t+1)] \cdot [x_{k+1}(t+1) - x_k(t+1)] = f_2[X, K(t+1), \xi_{k+1}(t), \xi_{k+1}(t+1), e_k(t+1)], \quad (\text{B16})$$

where $f_1(\cdot)$ and $f_2(\cdot)$ are functions of their arguments and $X = \{A, B, C, Q, R^{-1}\}$. If both $f_1(\cdot)$ and $f_2(\cdot)$ are set equal to 0, (B16) holds independently of system state and gives rise to the Riccati equation (53) and the difference equation (54), respectively. Finally, if $p_{k+1}(N) = 0$ and both $K(N)$ and $\xi_{k+1}(N)$ are also set equal to 0, (56) still holds independent of system state when $t = N$.

ACKNOWLEDGMENTS

This work was supported by the National Natural Science Foundation of China (Nos. 61773181, 61203092, 62103293), the Fundamental Research Funds for the Central Universities (No. JUSRP51733B), the Natural Science Foundation of Jiangsu Province (No. BK20210709), Suzhou Municipal Science and Technology Bureau (No. SYG202138), 111 Project (No. B23008), the National Science Centre in Poland (No. 2020/39/B/ST7/01487), and Postgraduate Research & Practice Innovation Program of Jiangsu Province (No. KYCX22_2306).

DATA AVAILABILITY STATEMENT

The data that support the findings of this study are available from the corresponding author upon reasonable request.

References

1. Arimoto S, Kawamura S, Miyazaki F. Bettering operation of robots by learning. *J Robot Syst.* 1984; 1(2): 123-140.
2. Bristow DA, Tharayil M, Alleyne AG. A survey of iterative learning control: a learning-based method for high-performance tracking control. *IEEE Control Syst Mag.* 2006; 26(3): 96-114.
3. Ahn HS, Chen Y, Moore KL. Iterative learning control: brief survey and categorization. *IEEE Trans Syst Man Cybern Part C.* 2007; 37(6): 1099-1121.
4. Tao H, Zhou L, Hao S, Paszke W, Yang H. Output feedback based PD-type robust iterative learning control for uncertain spatially interconnected systems. *Int J Robust Nonlinear Control.* 2021; 31(12): 5962-5983.
5. Bu X, Liang J, Hou Z, Chi R. Data-driven terminal iterative learning consensus for nonlinear multiagent systems with output saturation. *IEEE Trans Neural Netw Learn Syst.* 2020; 32(5): 1963-1973.
6. Blanken L, Willems J, Koekebakker S, Oomen T. Design techniques for multivariable ILC: application to an industrial flatbed printer. *IFAC-PapersOnLine* 2016; 49(21): 213-221.
7. Dekker LG, Marshall JA, Larsson J. Experiments in feedback linearized iterative learning-based path following for center-articulated industrial vehicles. *J Field Robot.* 2019; 36(5): 955-972.
8. Hao S, Liu T, Rogers E. Extended state observer based indirect-type ILC for single-input single-output batch processes with time- and batch-varying uncertainties. *Automatica.* 2020; 112: 108673.
9. Tao H, Paszke W, Rogers E, Yang H, Galkowski K. Iterative learning fault-tolerant control for differential time-delay batch processes in finite frequency domains. *J Process Control.* 2017; 56: 112-128.
10. Freeman CT, Hughes AM, Burridge JH, Chappell PH, Lewin PL, Rogers E. Iterative learning control of FES applied to the upper extremity after stroke. *Control Eng Pract.* 2009; 17(3): 368-381.
11. Hughes AM, Freeman CT, Burridge JH, Chappell PH, Lewin PL, Rogers E. Feasibility of iterative learning control mediated by functional electrical stimulation for reaching after stroke. *J Neurorehabil Neural Repair.* 2009; 23(6): 559-568.
12. Seel T, Werner C, Raisch J, Schauer T. Iterative learning control of a drop foot neuroprosthesis - generating physiological foot motion in paretic gait by automatic feedback control. *Control Eng Pract.* 2016; 48: 87-97.
13. Shi J, He X, Zhou D. Iterative learning control for nonlinear stochastic systems with variable pass length. *J Franklin Inst.* 2016; 353(15): 4016-4038.

14. Li X, Xu JX, Huang D. An iterative learning control approach for linear systems with randomly varying trial lengths. *IEEE Trans Autom Control*. 2014; 59(7): 1954-1960.
15. Li X, Shen D. Two novel iterative learning control schemes for systems with randomly varying trial lengths. *Syst Control Lett*. 2017; 107: 9-16.
16. Wei YS, Li XD. Robust iterative learning control for linear continuous systems with vector relative degree under varying input trail lengths and random initial state shifts. *Int J Robust Nonlinear Control*. 2021; 31(2): 609-622.
17. Liu S, Wang J, Shen D, O'Regan D. Iterative learning control for noninstantaneous impulsive fractional-order systems with varying trial lengths. *Int J Robust Nonlinear Control*. 2018; 28(18): 6202-6238.
18. Strijbosch N, Oomen T. Iterative learning control for intermittently sampled data: monotonic convergence, design, and applications. *Automatica*. 2022; 139: 110171.
19. Shen D, Zhang W, Wang Y. On almost sure and mean square convergence of P-type ILC under randomly varying iteration lengths. *Automatica*. 2016; 63: 359-365.
20. Meng D, Zhang J. Deterministic convergence for learning control systems over iteration-dependent tracking intervals. *IEEE Trans Neural Netw Learn Syst*. 2018; 29(8): 3885-3892.
21. Seel T, Schauer T, Raisch J. Monotonic convergence of iterative learning control systems with variable pass length. *Int J Control*. 2017; 90(3): 393-406.
22. Jin X. Iterative learning control for MIMO nonlinear systems with iteration-varying trial lengths using modified composite energy function analysis. *IEEE Trans Cybern*. 2021; 51(12): 6080-6090.
23. Shen D, Xu J. Robust learning control for nonlinear systems with nonparametric uncertainties and nonuniform trial lengths. *Int J Robust Nonlinear Control*. 2019; 29(5): 1302-1324.
24. Shen M, Wu X, Park JH, Yi Y, Sun Y. Iterative learning control of constrained systems with varying trial lengths under alignment condition. *IEEE Trans Neural Netw Learn Syst*. 2021: 1-7.
25. Ketelhut M, Stemmler S, Gesenhues J, Hein M, Abel D. Iterative learning control of ventricular assist devices with variable cycle durations. *Control Eng Pract*. 2019; 83: 33-44.
26. Liu C, Ruan X, Shen D, Jiang H. Optimal learning control scheme for discrete-time systems with nonuniform trials. *IEEE Trans Cybern*. 2022: 1-12. doi: 10.1109/TCYB.2022.3166558

27. Wang L, Li X, Shen D. Sampled-data iterative learning control for continuous-time nonlinear systems with iteration-varying lengths. *Int J Robust Nonlinear Control*. 2018; 28(8): 3073-3091.
28. Owens DH. *Iterative Learning Control: An Optimization Paradigm*. Springer London . 2016.
29. Chu B, Owens DH. Iterative learning control for constrained linear systems. *Int J Control*. 2010; 83(7): 1397-1413.
30. Chen Y, Chu B, Freeman CT. Generalized iterative learning control using successive projection: algorithm, convergence, and experimental verification. *IEEE Trans Control Syst Technol*. 2020; 28(6): 2079-2091.
31. Zhuang Z, Tao H, Chen Y, Stojanovic V, Paszke W. Iterative learning control for repetitive tasks with randomly varying trial lengths using successive projection. *Int J Adapt Control Signal Process*. 2022; 36(5): 1196-1215.
32. Sakai M. Strong convergence of infinite products of orthogonal projections in Hilbert space. *Appl Anal*. 1995; 59(1-4): 109-120.
33. Amann N, Owens D, Rogers E. Iterative learning control for discrete-time systems with exponential rate of convergence. *Control Theory Appl*. 1996; 143(2): 217-224.
34. Yoon D, Ge X, Okwudire CE. Optimal inversion-based iterative learning control for overactuated systems. *IEEE Trans Control Syst Technol*. 2020; 28(5): 1948-1955.